Desalination and Water Treatment
www.deswater.com
doi: 10.5004/dwt.2021.27478

231 (2021) 81–100
August

Investigation on a submarine reverse osmosis system assisted with the ocean thermal energy

Jiansheng Wang, Dingfan Zhang, Xueling Liu*

Key Laboratory of Efficient Utilization of Low and Medium Grade Energy, MOE, School of Mechanical Engineering, Tianjin University, Tianjin 300350, China, Tel. +86-22-27890053; emails: lxling@tju.edu.cn (X. Liu), jsw@tju.edu.cn (J. Wang), zhangdf_tju@foxmail.com (D. Zhang)

Received 23 October 2020; Accepted 20 May 2021

ABSTRACT

To reduce the energy consumption of the reverse osmosis desalination system, a submarine reverse osmosis conveyor (SRC) system was proposed. The conveyor that can utilize the ocean thermal energy to deliver the freshwater in the deep-sea replaces the freshwater pump in the conventional submarine reverse osmosis-pump (SRP) system. Firstly, the conveyor cycle was thermodynamically analyzed and the principles of the proposed system were illustrated. Secondly, a mathematical model describing the joint operation processes of the reverse osmosis (RO) components and the conveyor adopting the pressure boosting mode was established with four independent design parameters, that is, recovery rate, operating pressure, kinds of working fluids and boost ratio. Thirdly, the auxiliary pump power, the conveyor thermal efficiency and the specific electric energy consumption (SEC) were investigated on the relationships with the four independent parameters. Eight kinds of working fluids were selected out as candidates. The optimal design parameters were eventually obtained under different working conditions. Finally, the proposed system was compared with the SRP system as well as other energy-saving approaches for the RO process. Results showed that the power of the booster pump was the highest and account for around 50% of the total pump power. The SEC increased first and then decreased with the boost ratio growing. With the increase of the operating pressure or the decrease of the recovery rate, the SEC increased. The variations of the thermal efficiency were opposite to that of the SEC. At the typical recovery of 50%, the optimal SEC reached 1.39 kWh/m^3 with an operating pressure of 5.5 MPa. The optimal working fluid was R236fa with a boost ratio of 22.21. Compared with the SRP system, the SRC system reduced the SEC by 20%–30%. The proposed system could provide a potential approach to saving electric energy for seawater reverse osmosis desalination systems.

Keywords: Seawater reverse osmosis desalination; Hydrostatic pressure; Ocean thermal energy; Thermal water pump

1. Introduction

With social development and population growth, the stress of freshwater supply becomes greater and greater. Desalination has become a viable way to solve the problem of freshwater shortage. It is estimated that the current total installed capacity of seawater desalination is more than 90 million m^3/d, equivalent to 0.6% of the total global freshwater supply [1]. Nowadays desalination processes can be divided into two categories: phase change process and single-phase process. Multi-effect distillation (MED) and multi-stage flash (MSF) belong to the phase change process. The single-phase process mainly refers to reverse osmosis (RO) desalination. MED, MSF and RO are the main methods used all over the world [2–5]. The energy consumed per year by the desalination industry worldwide is

* Corresponding author.

estimated to be 75.2 TWh [6]. However, the cost of fossil fuels has been increasing and overuse of them has caused severe pollution.

Due to the relatively low energy cost, easy maintenance and compact structure, RO systems have already been accounted for the largest proportion (nearly 60%) among all methods of seawater desalination [7,8]. In RO systems, high-pressure pumps consume most of the required energy since the high operating pressure. In practice, the specific electric energy consumption (SEC) of the large and medium RO components coupled with energy-recovery devices was around 3–4.5 kWh/m^3 [9].

RO systems coupled with renewable energy sources could be a feasible approach to reducing the consumption of fossil fuels [10,11]. RO systems driven by solar energy and wind energy have been investigated extensively [12–15], and many of these systems have been applied in practice. Simultaneously, hydrostatic pressure can also be used to drive RO components. The idea of using the hydrostatic pressure to drive RO systems at a suitable working depth was firstly proposed in the 1960s [16,17]. Depending on the location of the RO components, RO systems driven by hydrostatic pressure can be divided into two types. One is the submarine RO system, in which the RO components are placed in the sea. The other is the underground RO system, and the RO components were placed at the location deep enough near the coast [18]. Hebden and Botha [19] early studied the feasibility of the deep seawater reverse osmosis desalination (SWRO) systems. The literature [20] had proved the technical feasibility of the submarine RO system through experiments in 1996. The experimental research on the submarine reverse osmosis-pump (SRP) system was implemented firstly by JRC Ispra and Energia TA-Florence in the Tyrrhenian Sea offshore between Corsica and Tuscany in 1996 [21]. A simplified experimental facility operated successfully at –550 m in real short-term operational conditions. The desalinated water quality was very good in comparison to the water produced in conventional RO plants as well as to commercial mineral water. The experiment verified the technical feasibility of the deep-sea water reverse osmosis concept. The literature Colombo et al. [22] introduced a submarine RO system, namely reverse osmosis deep-sea system (RODSS). It was theoretically calculated that when working depth was about 500 m and the freshwater production was 2×10^4 m^3/d, the specific electric energy consumption of the system was about 1.88 kWh/m^3, which was about 50% lower than that of the traditional RO system. Al-Kharabsheh [23] proposed a new type of RO system driven by hydrostatic pressure. The operating pressure of the RO assembly was provided by a sufficiently high water column. The entire system was placed above sea level and usually close to the mountain in order to provide a higher water column. The results of the energy analysis showed that the system required only 0.85 kWh of electric energy to produce freshwater per unit. Charcosset et al. [24] reviewed and compared various RO systems using hydrostatic pressure, including submarine, underground and adjacent mountain systems. The results confirmed that hydrostatic pressure could reduce the cost associated with the high-pressure pumps in the operation of the ground-based RO systems.

Thermal water pumps are the devices to deliver the water for agricultural irrigation, industry and residential requirements. Three types of thermal water pumps have been investigated. The first is vapor cycles based systems. Sharma [25] proposed a solar water pump. The experimental results showed that the discharge of the pump was 8.6 L/min at a 3 m head while it reduced to 3.62 L/min at a head of 6 m with a freon pressure of 2.4 mg/cm^2. Sumathy et al. [26] and Wong and Sumathy [27] proposed a novel solar thermal water pump system in which a solar vapor generator storage tank was induced. The global efficiency was between 0.12% and 0.14% [28]. It was also theoretically calculated that the system performance was better with ethyl ether as a working fluid instead of pentane [29,30]. The second is liquid piston systems. In those systems, the water lifting and suction are caused by the oscillation of a U-shape liquid column. The main disadvantage was the instability under changing loads [13]. In the system designed by Klerk and Rallis [31], the heating and cooling of the gas were separated into two chambers with the mobile piston. The system was able to deliver 54 L/h with the delivery head of 1 m. The third is hydride-based systems. When metal hydride was heated by a heat source, the hydrogen was generated and made the chamber expanding. While metal hydride was cooled, the hydrogen was adsorbed, which resulted in the reduction of the pressure inside the chamber and water suction. Debashis and Gopal [32] conducted an experiment on the proposed system in the Indian region of Kolkata. The temperature of metal hydride varied between 21.85°C and 61.85°C. The flow of water pumped was about 240 L/d and per kilogram metal hydride on a clear summer day.

Recently, Date and Akbarzadeh [33] proposed a new thermodynamic cycle for thermal power pumps. The device using acetone as a working fluid, which could provide sufficient water suction head of around 7 m with heat sink at 20°C and delivery head of around 35 m with a heat source at 100°C. Nihill et al. [34] conducted an experimental investigation on the thermal water pump based on the thermal power pump (TPP) cycle. A cylinder-piston device was created, which was more compact than that proposed by literature [33]. The results proved that up to 20 m head was obtained with the heat source at about 80°C. Nihill et al. [35] replaced the high-pressure pump with a thermal water pump in the brackish water RO desalination system. The experimental results showed that the proposed system could produce freshwater at a rate of 1.27 L/h with a specific energy consumption of 165 MJ/m^3 for the heat source at 86°C, and the feed brackish water salinity at 1184 ppm. In addition, there were also some investigations on the RO systems coupled with Stirling engines [36,37].

Combining the submarine RO system with the thermal water pump, a novel submarine reverse osmosis conveyor (SRC) system is proposed in the present work. As mentioned above, in previous submarine RO-pump systems, the freshwater produced in the deep sea was transported to sea level by delivery pumps. To reduce the electric energy consumed by the submarine RO system, the ocean thermal energy (temperature difference energy) is used to replace the pump to deliver the freshwater. The working cycle of the conveyor using ocean thermal energy under specific operating

conditions is probed. Subsequently, the optimization scheme combining the RO components and conveyor is investigated as well. The SEC of three systems, namely the SRC system, the SRP and the ground-based reverse osmosis (GBR) system, is compared and discussed.

2. Principle of RO systems

2.1. Ground-based RO system

The ground-based RO system consists of pretreatment components, the high-pressure pump, and RO components. As shown in Fig. 1, the pretreated seawater is piped to the RO components by a high-pressure pump, then separated into fresh water and brine by the RO membranes.

As shown in Fig. 2a, multiple membrane elements are usually connected in series and parallel to overcome the inefficiency of individual membrane elements. Several membrane elements in series are placed in a pressure container as shown in Fig. 2b. The pressure container can increase the recovery of each individual membrane element. Multiple pressure containers in parallel form a stage of the RO components as shown in Fig. 2c. Pressure containers connected in parallel increase the produced water flow. The water produced by a stage of RO components can be used as the feed water for the next stage of RO components, thereby reducing the salinity of the produced water, and improve the recovery rate.

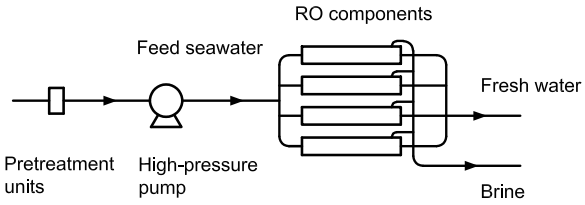

Fig. 1. Schematic of the ground-based RO system.

The operating pressure of the RO components is affected by various factors such as temperature, average water flux, the salinity of feed water, recovery rate, type of membrane elements and so on. Meantime, the recovery rate is affected by factors such as the salinity of the feed water, operating pressure, content of scaling ions, the type of membrane elements and so on. The operating pressure of seawater desalination is generally 5.5~8 MPa, and the recovery rate is 50%–90%.

2.2. Submarine RO-pump system

The structure of the submarine RO-pump system is shown in Fig. 3. The RO components are placed near the offshore in sufficient depth to provide the required operating pressure. The freshwater produced in the deep sea is then pumped to sea level. The idea of using the hydrostatic pressure to drive RO systems at a suitable working depth was firstly proposed in the 1960s [16,17].

2.3. Submarine RO-conveyor system

As shown in Fig. 4, the submarine RO-conveyor system is mainly composed of RO components and the conveyor is located on the seafloor with sufficient depth and protected by the containers with atmospheric pressure. The operation pressure of RO components is provided by the hydrostatic pressure of the local seawater. Thus, high-pressure pumps used in ground-based RO systems could be saved. The produced freshwater with atmospheric pressure is delivered to sea level by a conveyor. Concentrated brine is discharged into the sea. The whole process can be divided into seawater desalination process and freshwater delivery process. The detailed operating processes would be illustrated in Section 3.

Specifically, the conveyor of the present RO-conveyor system is a cylinder-piston device, which can convert ocean thermal energy into mechanical energy. The seawater

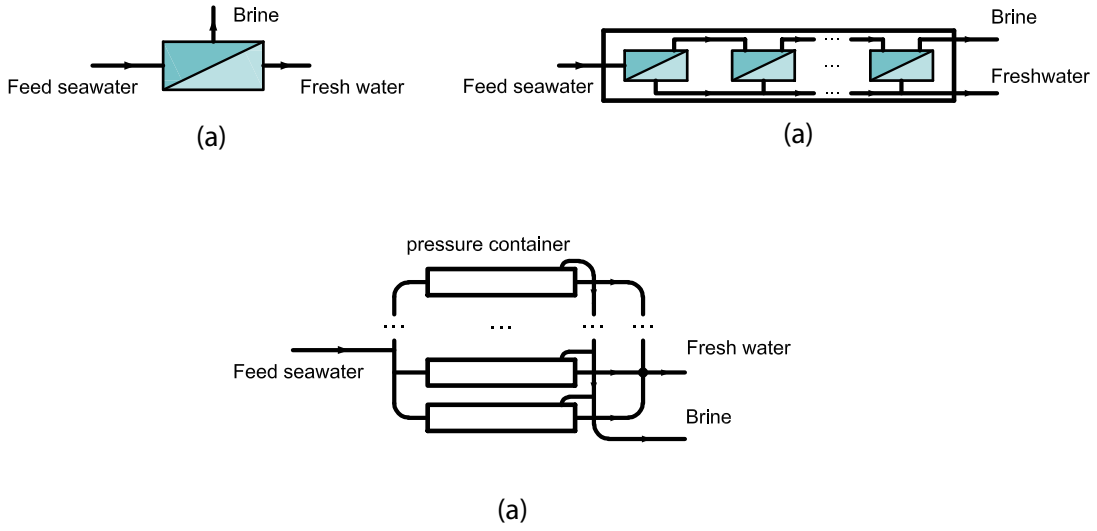

Fig. 2. The arrangement of the membrane elements: (a) membrane element, (b) pressure container, and (c) a stage of the RO components.

temperature varies with the depth, so the seawater temperature difference is used to deliver the freshwater via the conveyor. In the present conveyor, the surface seawater is used as the hot reservoir, and the local seawater of the working place is used as the cold reservoir. The working fluid absorbs heat from the hot reservoir and evaporates to push the piston upwards to deliver the produced freshwater to sea level. The working fluid vapor is cooled by the local seawater to the liquid state, which is ready for the next conveyor cycle.

Auxiliary pumps are required in the proposed system. A circulation pump is used to overcome the resistance loss of RO components. The booster pump is used to increase the pressure of freshwater to the condensing pressure. The heat source pump is used to overcome the resistance losses in the surface seawater pipelines and the heat transfer device of the conveyor. The electric energy consumed by auxiliary pumps comes from the grid or other energy sources such as photovoltaics and wind turbines.

RO components, the conveyor and auxiliary pumps are all placed in two closed containers which are used to provide structural support for the working environment. The pretreatment method should be determined according to the local seawater properties, such as pH, organic and inorganic compound composition, quantity of anaerobic bacteria and total dissolved solids and so on [21]. Due to the better water quality in the deep sea, the pretreatment units usually are simpler than that of the ground-based RO system.

3. Conveyor cycle

3.1. Working processes of the conveyor

As shown in Fig. 5, the conveyor is a cylinder-piston device. The heat exchanger which consists of a flat plate condenser and a flat plate evaporator is placed at the bottom of the cylinder. The working fluid is filled in the cylinder below the piston. The surface seawater and the local seawater alternately flow through the heat exchanger. Correspondingly, the working fluid evaporates and condensates alternately. The volumetric work done by the working fluid during evaporation is used to deliver the freshwater.

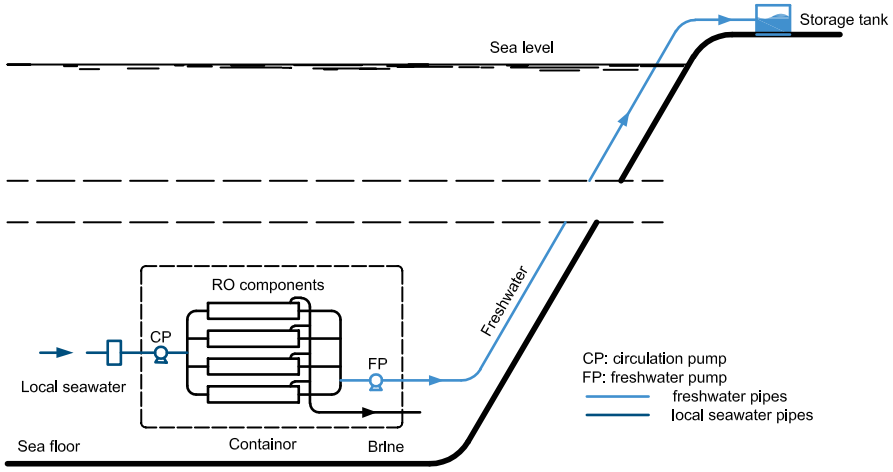

Fig. 3. Schematic of the SRP system.

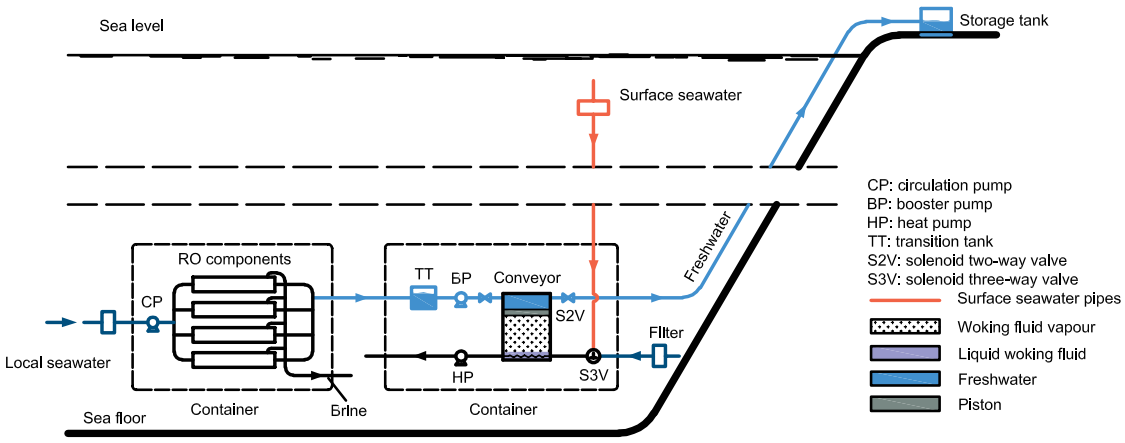

Fig. 4. Schematic of the SRC system.

According to the specific application scenario, the combination of delivery head, heat source temperature and the type of working fluids should be considered in the design of the conveyor [33]. The operation pressure of the seawater RO system was around 5.5–8 MPa due to the high salinity of seawater [9]. Therefore, the working fluids in the conveyor should be evaporated under 5.5~8 MPa at the surface seawater temperature (SST) around 25°C~30°C. However, the SST is too small to evaporate most kinds of working fluids under 5.5~8 MPa. Thus, the pressure boosting mode of the conveyor is designed as shown in Fig. 6. The two pistons with different diameters are connected by a rigid structure so that they can move up and down synchronously. When the diameter of the piston below is larger, the evaporation pressure received by the upper piston is amplified. Thus, under the same operating pressure, the evaporation pressure in the pressure boosting mode conveyor is smaller. When the pressure of the water-side was less than atmospheric pressure [35,36], the conveyor can draw water that was lower than its own position with the aid of atmospheric pressure.

3.2. Thermodynamic cycle of the conveyor

The pressure boosting mode of the conveyor can adapt to the wider combination of heat source, working fluids and delivery height. The pressure ratio of the upper piston to the piston below is defined as the boost ratio of the conveyor, which is denoted by the symbol r, namely:

$$r = \frac{P_w}{P_{\mathrm{wf}}} = \frac{S_{\mathrm{wf}}}{S_w} = \left(\frac{d_{\mathrm{wf}}}{d_w}\right)^2 \tag{1}$$

where S is the bottom area of the piston and d is the diameter of the piston.

The T-S and P-v diagrams of the conveyor cycle are shown in Fig. 7. The operating processes of the conveyor subsystem are illustrated in Fig. 8. When the working fluid reaches the saturated liquid state at point 4, the local

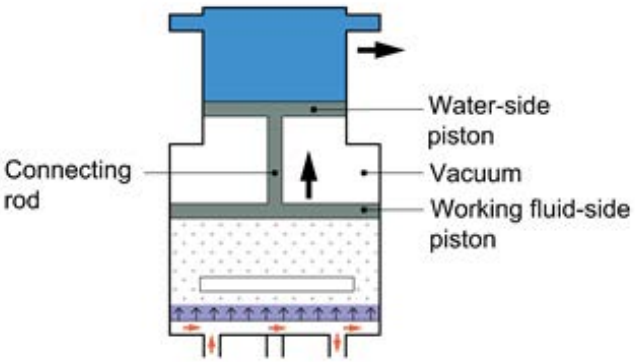

Fig. 6. Schematic of the conveyor.

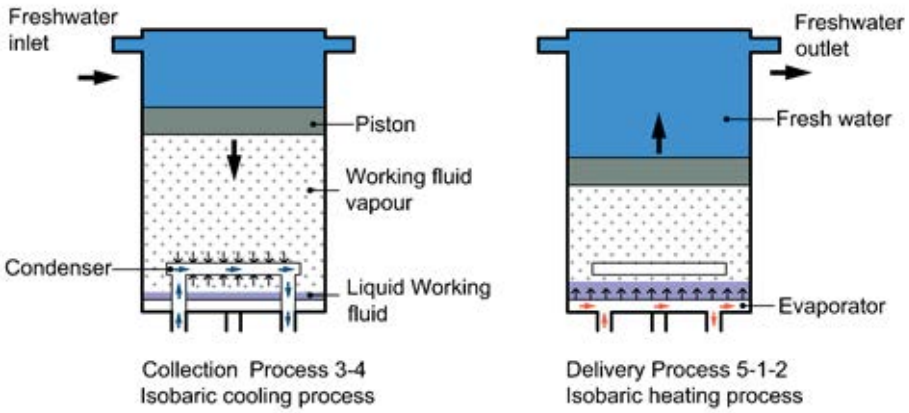

Fig. 5. Cross-sections of the conveyor through two different planes.

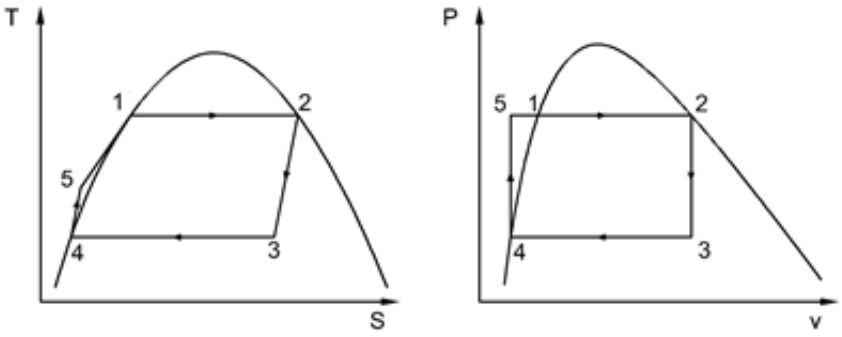

Fig. 7. T-S and P-v diagrams of the conveyor cycle.

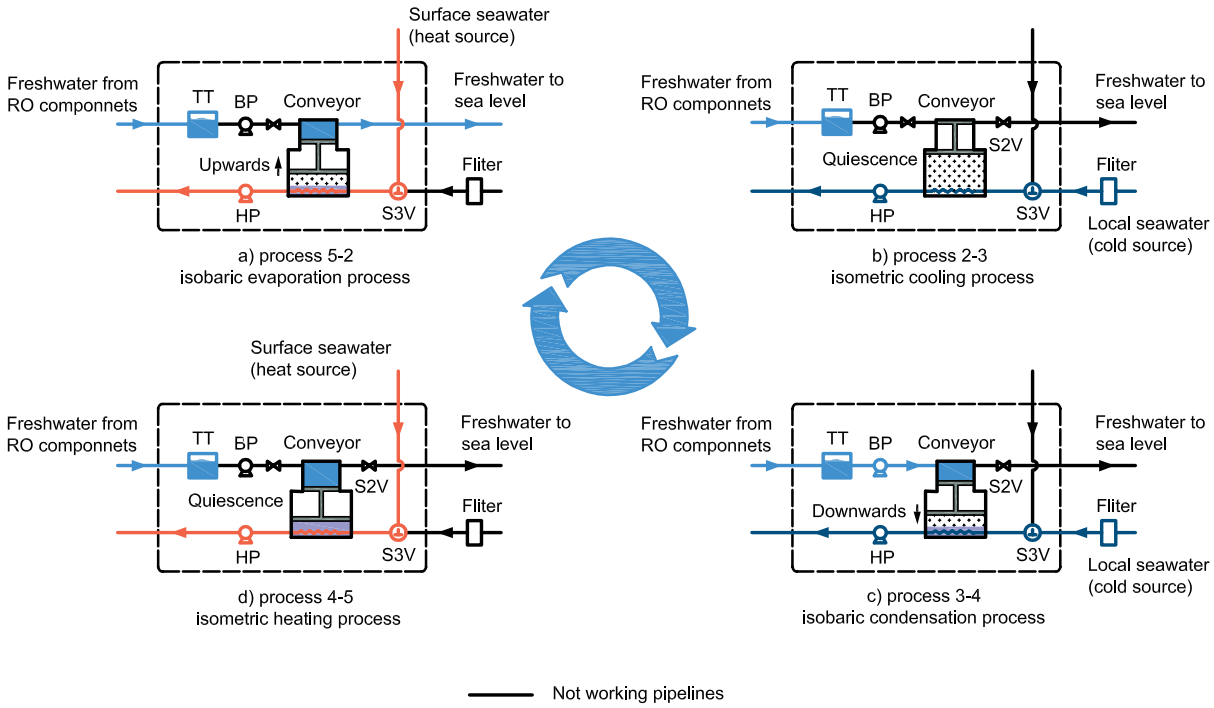

Fig. 8. Operating scheme of the conveyor subsystem.

seawater is stopped by the S3V and the surface seawater flows into the heat exchanger of the conveyor. In addition, the freshwater inlet valve is closed and the booster pump stops working. As the working fluid absorbs heat from the surface seawater, the pressures of the working fluid and the upper piston increase. While the piston remains quiescence until the working fluid reaches the state at point 5. Because the upper piston pressure is lower than the delivery pressure. Thus, process 4-5 is the isomeric heating process. At point 5, the freshwater outlet valve opens and the piston begins to move upwards with the working fluid evaporating. It is assumed that the working fluid was heated to the saturated vapor state at point 2. Thus, the piston stops moving upwards when the working fluid reaches the state at point 2. Process 5-2 is the isobaric evaporation process. At point 2, freshwater outlet valve is closed and the surface seawater is stopped by the S3V. Simultaneously, the local cold seawater flows into the condenser of the conveyor. Hence the working fluid starts to be cooled and its pressure starts to decrease. The working fluid temperature is the minimum at point 3 under the conditions of the cold source and the condenser. Compared to the working fluid pressure, the pressure applied by the piston to the working fluid can be neglected. During the process 2-3, the pressure and temperature of the working fluid in a wet steam state decrease while the working fluid volume remains constant and the piston remains quiescence. Thus, process 2-3 is the isomeric cooling process. At point 3, the freshwater inlet valve opens and the booster pump starts up. The freshwater in the transition tank is pressurized by the booster pump from the atmospheric pressure to the working fluid pressure and flows into the cylinder. Thus, the working fluid condensates under the pressure at point 3. It is assumed that the working fluid is cooled to the saturated liquid state at point 4. Process 3-4 is the isobaric condensation process. So far, a cycle is completed.

In summary, the conveyor cycle consists of an isobaric evaporation process 5-2, an isomeric process 2-3, an isobaric condensation process 3-4 and an isomeric process 4-5. During the isobaric evaporation process 5-2, the piston moves upwards and the freshwater is delivered. During the process 3-4, the piston moves downwards and the freshwater is collected. The booster pump is essential for the conveyor cycle because of the high pressure of the working fluid when condensation.

The mechanical work is exported during the isobaric evaporation process in the conveyor cycle. While it is exported during the isothermal process in the general power cycles. Additionally, the working fluid flows in the general power cycles while does not flow in the conveyor cycle. Date and Akbarzadeh [33] found that the ideal cycle performance of the thermal water pump was about 40%, when the driving temperature difference was 60°C and acetone was used as the working fluid.

4. Thermodynamic analysis

4.1. RO components

Due to the great seawater salinity and osmotic pressure, SWRO desalination operated at 5.5~8 MPa [38]. In the present work, operating pressure and recovery rate are taken into account and regarded as independent variables. Thus, the selection of RO membranes and the arrangement of RO stages should be determined by the two parameters. The variation of the recovery rate with the local seawater

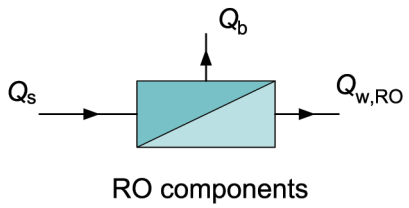

Fig. 9. Illustration of the fluid flow in the RO components.

temperature is ignored. In the RO components as shown in the Fig. 9, the volumetric flow of the feed seawater Q_s is equal to the sum of the concentrated brine flow Q_b and the product water flow $Q_{w,\mathrm{RO}}$, namely:

$$Q_s = Q_{w,\mathrm{RO}} + Q_b \tag{2}$$

The recovery rate of RO components is defined as the ratio of fresh water flow to feed seawater flow, thus,

$$Y = \frac{Q_{w,\mathrm{RO}}}{Q_s} \tag{3}$$

According to the international high-pressure seawater equation of state [39], the density of the deep seawater is the function of the salinity, pressure and temperature. Thus,

$$\rho = \frac{\rho(S,T,O)}{\left(1 - P/K(S,T,P)\right)} \tag{4}$$

where $\rho(S,T,O)$ was the international seawater equation of state at atmospheric pressure in 1980, P is the seawater pressure and $K(S,T,P)$ is the secant bulk modulus.

The average density of the seawater above a certain depth in the sea can be obtained by:

$$\bar{\rho} = \frac{(\rho_c + \rho_s)}{2} \tag{5}$$

where ρ_s is the surface seawater density and ρ_c is the density of the seawater at a certain depth.

As shown in the Fig. 10, the operating pressure of the RO components is provided by the seawater hydrostatic pressure, thus,

$$P_{\mathrm{op}} = P_{\mathrm{atm}} + \bar{\rho} g D \tag{6}$$

where D stands for the working depth of the RO components.

4.2. Conveyor cycle

The performance of the conveyor was closely related to various factors such as the temperature of the cold and heat source, the kinds of working fluids and boost ratio, etc. [33]. The effects of the working fluids and the boost ratio on the performance of the conveyor are investigated in this work. In the cylinder-piston device, the mass of working fluid is determined by the expandable volume of working fluids ΔV_1 as shown in the Fig. 11, and the difference of specific volume between the saturated steam and saturated liquid. The mass of working fluid in the conveyor cycle can be obtained by the following formula:

$$m_{\mathrm{wf}} = \frac{\Delta V_1}{(v_2 - v_5)} \tag{7}$$

Since the RO components continuously produce fresh water and the conveyor delivers freshwater intermittently, the transitional tank is used to store freshwater that has not been delivered temporarily. When the system runs in steady-state, the amount of the freshwater delivered by the conveyor within 1 d $|Q_{w,d}|$ (m^3) should be equal to that of the freshwater produced by the RO components $|Q_{w,\mathrm{RO}}|$. The number of cycles within 1 d is determined by the $|Q_{w,d}|$ and the delivery volume per cycle ΔV_2. Hence,

$$n = \frac{|Q_{w,d}|}{\Delta V_2} \tag{8}$$

In 1 d, the ratio of the total absorbing time of working fluid t_h (d) to the total releasing time of working fluid t_c is defined as t, namely:

$$t = \frac{t_h}{t_c}$$
$$t_h + t_c = \tag{9}$$

During each endothermic or exothermic process of the working fluid, the piston does not move during a period of time, that is, the 4-5 process and the 2-3 process as shown in Fig. 7. During these two processes, the specific volume of working fluid does not change while the pressure varies. The truly volume flow of the fresh water Q_w is the ratio of the total delivery volume $|Q_{w,d}|$ to the total delivery time within a day, thus,

$$Q_w = \frac{|Q_{w,d}|}{t_h} = \frac{|Q_{w,d}|(t+1)}{t} \tag{10}$$

When the piston moves upwards, the pressure of the upper piston can be calculated by the Bernoulli equation, namely:

$$P_w = \rho_w g D + \Delta P_f + P_{\mathrm{atm}} \tag{11}$$

where ΔP_f is the frictional resistance loss of the pipeline, which is composed of the on-way resistance and the local resistance. It can be calculated by the following formula:

$$\Delta P_f = \frac{\lambda L v^2 \rho}{2 d_n} + \frac{\xi v^2}{2g} \tag{12}$$

Therefore, the evaporation pressure of the working fluid is expressed as:

$$P_{\mathrm{evp}} = \frac{P_w}{r} \tag{13}$$

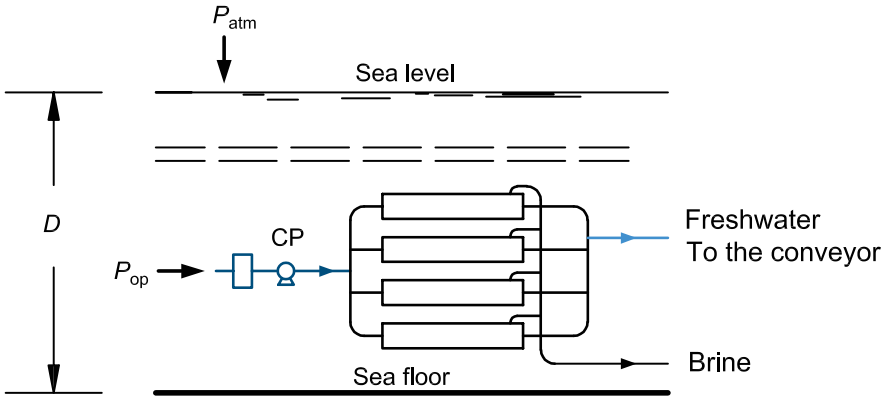

Fig. 10. Illustration of the origin of the operating pressure.

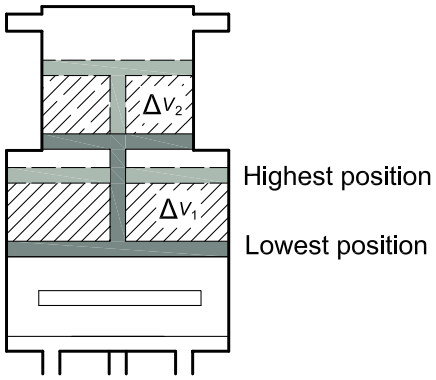

Fig. 11. Illustration of the principles of the boosting mode.

P_w is the threshold pressure at which the freshwater outlet valve opens. During isochoric endothermic process (process 4-5), the pressure of the working fluid increases. While the specific volume of the working fluid does not change and the piston remains quiescence, namely $v_4 = v_5$. Therefore, all of the absorbed heat is used to increase the inner energy of the working fluid, namely:

$$Q_{4\text{-}5} = m_{\text{wf}}\left(u_5 - u_4\right) \tag{14}$$

After the outlet valve opened, the working fluid begins to expand under a constant pressure P_w. The piston moves upwards and the freshwater is delivered to the sea level. Therefore, the heat absorbed in the process 5-2 can be obtained as:

$$Q_{5\text{-}2} = m_{\text{wf}}\left[u_2 - u_5 + P_{\text{evp}}\left(v_2 - v_5\right)\right] \tag{15}$$

The total heat absorbed by the working fluid in 1 d is equal to the amount of absorbed heat in a cycle multiplied by the number of cycles. Thus,

$$Q_{\text{absorb}} = n \cdot \left(Q_{4\text{-}5} + Q_{5\text{-}2}\right) \tag{16}$$

The surface seawater is served as the heat source of the conveyor. The evaporator inlet temperature is equal to the SST. It is supposed that the outlet temperature of the heat source is equal to the evaporation temperature of the working fluid. Then the heat absorbed by the working fluid in a day can be also obtained as:

$$Q_{\text{absorb}} = \rho_s \left|Q_h\right| c_p (T_{\text{hi}} - T_{\text{evp}}) \tag{17}$$

where $|Q_h|$ represents the total required surface seawater volume within a day.

The truly flow of the surface seawater is equal to the ratio of the total volume to the total heating time in a day, namely:

$$Q_h = \frac{\left|Q_h\right|}{t_h} = \frac{\left|Q_h\right|\left(t+1\right)}{t} \tag{18}$$

During the condensation process, the booster pump head is calculated as:

$$P_b = rP_{\text{con}} \tag{19}$$

Similar to the heating process, the total released heat in the cooling process within 1 d can be obtained as the following:

$$Q_{\text{release}} = n \cdot m_{\text{wf}}\left[u_2 - u_4 + P_{\text{con}}\left(v_2 - v_4\right)\right] \tag{20}$$

According to the energy conversion law, the total released heat can also be obtained as:

$$Q_{\text{release}} = \rho_c \left|Q_c\right| c_p \left(T_{\text{con}} - T_{\text{ci}}\right) \tag{21}$$

4.3. System performance

The performance of the proposed system is influenced by the total power consumption of auxiliary pumps. The circulation pump overcomes the pressure loss in RO

components, so the power consumption of the circulation pump can be expressed as:

$$W_{\text{cir}} = \frac{\Delta P_{\text{RO}} Q_s}{\eta} \tag{22}$$

where ΔP_{RO} is the pressure loss in RO components.

When the working fluid is heated, the surface seawater is supplied to the evaporator of the conveyor through the long pipeline by the heat source pump. Thus, the resistance loss of the pipeline should be considered. The head of the heat source pump can be obtained by Bernoulli's equation as following:

$$\Delta P_h = (\bar{\rho} - \rho_s) g D + \Delta P_f + \Delta P_{\text{evp}} - P_{\text{atm}} \tag{23}$$

where ΔP_{evp} is the pressure loss in evaporator.

The power consumption of the heat source pump when heating is obtained as:

$$W_h = \frac{\Delta P_h \left| Q_h \right|}{\eta} \tag{24}$$

The heat source overcomes the pressure loss in the condenser, so the heat source pump power is obtained as:

$$W_c = \frac{\Delta P_{\text{con}} \overline{Q_c}}{\eta} \tag{25}$$

The booster pump power can be obtained as:

$$W_b = \frac{P_b \left| Q_{w,d} \right|}{\eta} \tag{26}$$

The thermal efficiency of the conveyor can be represented as:

$$\eta_c = \frac{\left(P_w \Delta V_2 - \left(W_{\text{cir}} + W_h + W_c + W_b \right) \right)}{\left(Q_{\text{absorb}} - Q_{\text{release}} \right)} \tag{27}$$

Therefore, the specific electric energy consumption of the proposed system is obtained as:

$$\text{SEC}_1 = \frac{\left(W_{\text{cir}} + W_h + W_c + W_b \right)}{\left| Q_{w,\text{RO}} \right|} \tag{28}$$

The SEC of the proposed system is compared with that of two other RO systems under the same conditions. The first is the SRP system as shown in Fig. 3, which also uses seawater hydrostatic pressure as the operating pressure of RO components. While the produced freshwater is lifted by the freshwater pump to the sea level instead of the conveyor. The energy consumption of the freshwater pump can be obtained as:

$$W_w = \frac{\left(\rho_w g D + \Delta P_f + P_{\text{atm}} \right) \left| Q_{w,\text{RO}} \right|}{\eta} \tag{29}$$

Thus, the energy consumption of SRP system can be obtained by:

$$\text{SEC}_2 = \frac{\left(W_{\text{cir}} + W_w \right)}{\left| Q_{w,\text{RO}} \right|} \tag{30}$$

The other is the GBR system without the energy-recovery device. The high-pressure pump provides the operating pressure of RO components. The specific energy consumption is obtained as:

$$\text{SEC}_3 = \frac{P_{\text{op}} Q_s}{\left(\eta \left| Q_{w,\text{RO}} \right| \right)} \tag{31}$$

5. Results and discussion

In the present work, the operating pressure and the recovery rate of the RO components, as well as the boost ratio and kinds of the working fluids are selected as the independent variables. The united operation of the RO components and the conveyor is investigated. In addition, the SEC of the proposed system is compared with those of the SRP system and the GBR system.

Due to the lower temperature of the surface seawater, the temperature difference between the heat source and the working fluid is assumed to be within 10°C. The temperature difference between the inlet and the outlet of the heat source is set to 2°C or higher. The outlet temperature of surface seawater is greater than 0°C to prevent condensation. The volumetric flow of the freshwater produced by the RO components is assumed to be 100 m^3/d. The working place is located at the 20° north latitude of the Pacific Ocean. The ocean thermal energy in this area is rich, which is conducive to the efficient operation of the system. Simultaneously, the SST varies slightly with the day, night, and season, which makes it convenient to investigate the sensitivity of the system performance to the SST. The physical properties of the seawater are based on Argo data [40].

Fig. 12 shows the monthly average temperature of the seawater at the working place with 550 d bar. As shown in Fig. 12, the SST varies between 25°C–29.5°C, while the local seawater temperature changes within 1°C. Similarly, the salinity of surface seawater varies from approximately 34,600–35,100 ppm, and the salinity of local seawater stabilizes at approximately 34,140 ppm. Thus, the annual average temperature and salinity are used to calculate the density of local seawater. According to the international high-pressure seawater equation of state, as shown by Eq. (21), the density of the local seawater is determined by the local pressure. The power of the heat source pump, the thermal efficiency of the conveyor and SEC are all influenced by the heat source (surface seawater) temperature, which varies with the month as shown in Fig. 12.

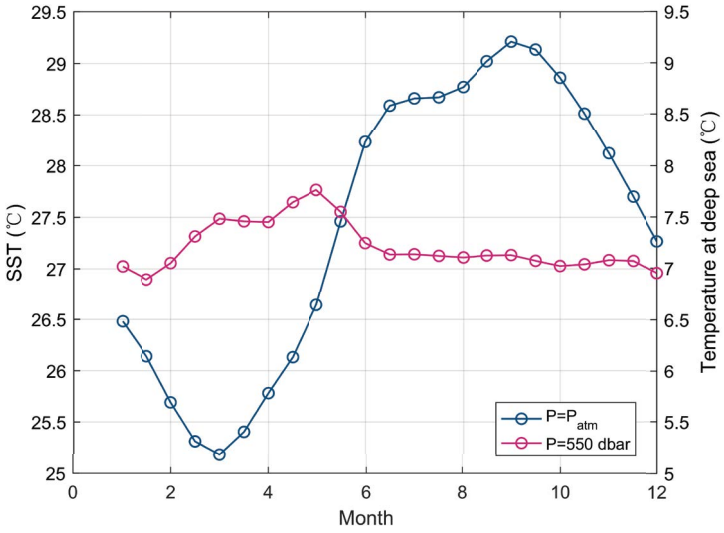

Fig. 12. The monthly average temperature of the seawater is 20° north latitude of the Pacific Ocean.

Without a special statement, 12-month averages of the performance parameters are used in this paper.

The boost ratio is selected as one of the optimal parameters. On the one hand, the increase of the boost ratio can reduce the evaporation temperature of the working fluid under the same operating pressure of RO components. Thus, the temperature difference between the working fluids and the heat source increases, and the power consumption of the heat source pump reduces. On the other hand, the augment of boost ratio increases the pressure of the booster pump during condensation. Therefore, the boost ratio has an optimum value that corresponding to the minimum SEC.

The properties of the working fluids have an important influence on the performance of the conveyor and also be regarded as the optimal parameter. The condensing temperature of the working fluids is assumed to be 10°C. To ensure the normal operation of the conveyor, the candidate working fluids should not react with the cylinder-piston device and should be insoluble in water. The candidate working fluids and their properties which are obtained by Refprop 9.0 are shown in Table 1 [41]. Meanwhile, global warming potential (GWP) and the ozone depression potential (ODP) which represents the impact of the working fluids on the environment are listed as well.

The working fluid and boost ratio should be considered to enable the conveyor to run normally. The time of the endothermic and exothermic processes in the conveyor is the same in this work. The parameters of the proposed system are shown in Table 2. The algorithm flow chart is shown in Fig. 13.

Fig. 14 shows the filling mass of the working fluid varies with the boost ratio and operating pressure. The selected working fluid is acetone. The recovery rate is 50%. Without the special statement below, the type of working fluid and the recovery rate remains unchanged. The results discussed below are also suitable for the other candidate working fluids and recovery rates. As the results show, the boost ratio has a slight influence on the filling mass. With the boost ratio increasing from 187.6 to 222.6, the filling mass of the acetone increases only from 8.863 to 8.957 kg. The filling mass increases linearly with the operating pressure increasing. Because, for the acetone, the ratio of the specific volume of saturated steam to saturated liquid decreases with the increase of evaporation pressure.

Fig. 15 shows the powers of auxiliary pumps in the SRC system and the freshwater pump in the SRP system vary with the boost ratio. The circulation pump is not included, of which the power is only determined by the recovery rate whether in the SRP or SRC. When the freshwater flow is 100 m^3/d, the W_{cir} decreases from 2.72 to 0.34 kW as the recovery rate increases from 10% to 80%. At a certain P_{op}, the evaporation pressure of the working fluid decreases with the increase of the r. The minimum of the r should ensure the evaporation temperature T_{evp} less than the critical temperature of the working fluid and the temperature difference between the T_{evp} and the heat source inlet temperature more than 2°C. The maximum should ensure the temperature difference between the T_{evp} and the heat source inlet temperature more than 10°C, which keeps the working fluid in the natural boiling state. As shown in Fig. 15a, the BP power increases with the boost ratio, because the growth of the boost ratio increases the water-side piston pressure during condensation. The power of the HP when cooling changes hardly with the boost ratio. Because the filling mass of the working fluid changes hardly as shown in Fig. 14 and the condensation pressure is constant in this work. While the HP power (when heating) decreases obviously with r increasing. The reason is that the evaporation temperature decreases with r increasing and the temperature difference of heat transfer increases. Thus, the heat source flow decreases.

Since HP power and BP power change in opposite trends with r, there must be an optimal boost ratio, which makes the total power of the HP pump and BP pump (the conveyor power) lowest at a certain P_{op}. Due to the constant power of the circulation pump, the total power of the SRC system or SEC will also be optimal. As shown in Fig. 15b, the conveyor power decreases first and then increases with

Table 1
Properties of candidate working fluids

Working fluids	Critical temperature T_{crit} (K)	Critical pressure P_{crit} (MPa)	GWP (100 y)	ODP	Type
R1234ze	382.52	3.64	6	0	Isentropic
R124	395.42	3.62	620	0.026	Isentropic
R142b	410.26	4.06	0.36	0.043	Isentropic
R152a	386.41	4.52	2.8	0	Wet
R218	345.02	2.64	5,700	0	Isentropic
R236fa	398.07	3.20	0.63	0	Isentropic
Acetone	508.10	4.7	–	–	Isentropic
RC318	388.38	2.78	9,100	0	Isentropic

Table 2
Parameters of the SRC system

Parameters	Symbol	Value
Freshwater production rate	Q_w	100 m^3/d
Condensation temperature	T_{con}	10°C
Inner diameter of pipes	d_n	100 mm
Ratio of heating time to cooling time	t	1
Pump efficiency	η	85%
Length of fresh water pipes	L	2D
Brine density	ρ_b	1,030 kg/m^3
Surface seawater density	ρ_s	1,025 kg/m^3
Freshwater density	ρ_w	1,000 kg/m^3
Pressure loss in RO components	ΔP_{RO}	0.2 MPa
Pressure loss in the conveyor	ΔP_{co}	0.03 MPa
Cycle numbers	n	24 × 60 d^{-1}

r increasing. When r is 207.6, the conveyor power is a minimum of 4.943 kW. Besides, it can be seen that the freshwater pump (FP) power is always greater than the conveyor power. Therefore, the SEC of the SRC system is smaller at 5.5 MPa.

Fig. 16 shows the minimum of auxiliary pump power varies with the operating pressure and the comparison to the FP power. The HP power (when cooling) changes hardly with the P_{op}. Although the temperature of the local seawater decreases with the P_{op} increasing, it's very limited to reduce the HP power (when cooling). The minimum HP power (when heating) increases with the P_{op} increasing. One reason is that the increase of P_{op} increases the work needed to deliver the freshwater. The other is that the temperature difference between the heat source and the working fluid reduces and thus heat source flow increases.

The minimum of the available r at a certain P_{op} should increase with the growth of P_{op} to ensure the temperature difference between the SST and T_{evp} more than 2°C as talked above. When the condensation pressure is constant, the BP power increases with r as shown in Fig. 15. Therefore, the minimum of BP power increases with the minimal r increasing.

The conveyor power increases with the P_{op} while is always less than the FP power of the SRP system as shown in Fig. 16b. Combining Figs. 15b and 16b, it can be concluded that the electric energy consumption per unit freshwater of the SRC system is lower than that of the SRP system at each P_{op}.

The variations of the thermal efficiency of the conveyor and the SEC of the whole system are displayed in Fig. 17. As talked about earlier, r has an optimal value that makes the SEC lowest. The SEC decreases first and then increases with the r increasing. When the r is 207.6, the SEC reaches the minimum of 1.317 kWh/m^3. At the same time, η_c reaches a maximum of 10.2%. It's obvious that η_c and SEC vary in opposite trends with r. Because the higher the η_c, the higher the proportion of ocean thermal energy in the total energy required during the delivery process. Thus, boosting the thermal efficiency of the conveyor is an important method for reducing the SEC. It is worth noting that although the η_c is negative at the r of around 187.6~190, the SEC of the SRC system is still smaller than 1.923 kWh/m^3 which is the SEC of the SRP system at the same conditions (P_{op} = 5.5 MPa, Y = 50%). In other words, the sum of HP power and BP power, which is larger than the mechanical work done by the conveyor though, is still lower than the power of the freshwater pump in the SRP system.

The results shown in Fig. 18 demonstrate that the optimal SEC increases and $\eta_{c,opt}$ decreases with the increase of P_{op}. Because the total power consumption of the auxiliary pumps increases as displayed in Fig. 16. Combining Figs. 17 and 18, it can be concluded that the optimal SEC is 1.316 kWh/m^3 under the working conditions of 5.5 MPa operating pressure and 50% recovery rate when acetone is used as the working fluid and boost ratio is 207.6. Simultaneously, the optimal thermal efficiency of the conveyor reaches 10.19%.

Fig. 19 shows the monthly SEC when the 12-month average SEC is optimal under different P_{op}. Comparing Fig. 12 with Fig. 19a, it can be seen when the SST reaches the highest value in September, the SEC falls the minimum. The SEC is relatively stable from June to October while fluctuates intensely from January to May. With the increase of the P_{op}, the fluctuation range of the SEC over the whole year enlarges. As Fig. 19b shows, the SEC decreases with the increase of the SST and the absolute slope also decreases. Thus, the lower the SST, the more sensitive the SEC. It is more suitable for the SRC system to operate in sea areas with high SST.

Fig. 20 shows the optimal boost ratio for the candidate working fluids and corresponding optimal SEC under different operating pressures. Because of the excessive boost

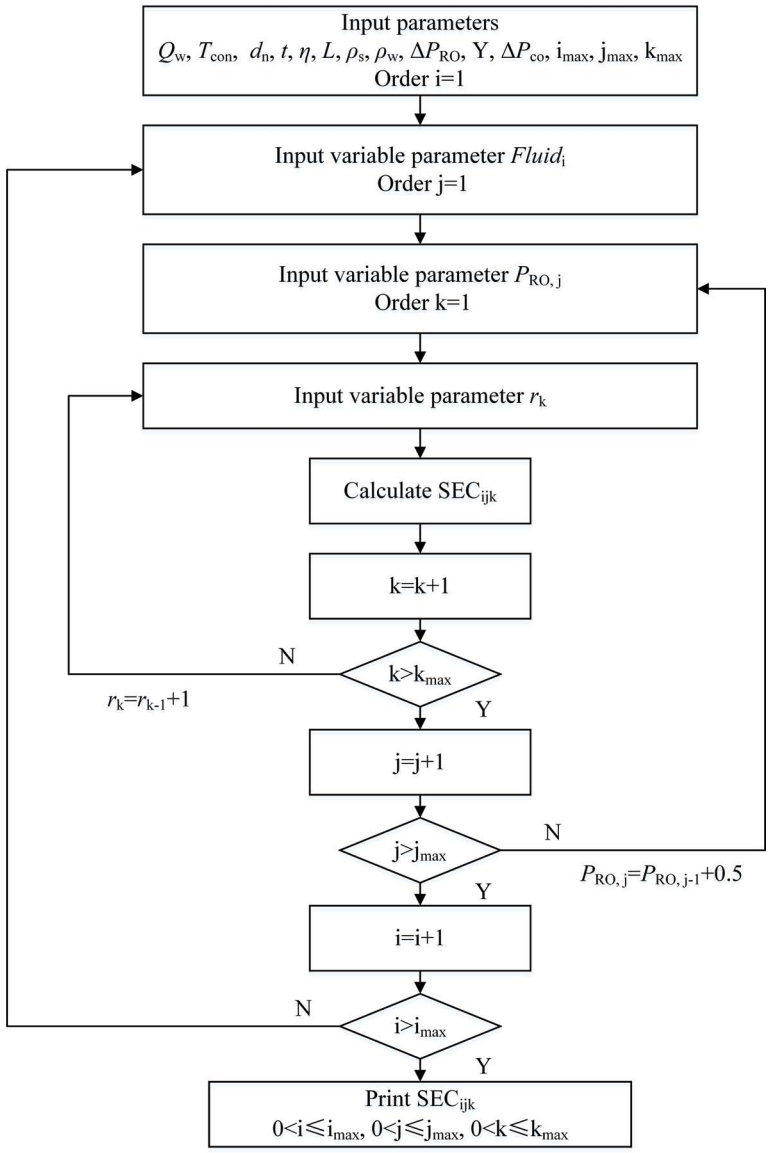

Fig. 13. Flowchart of optimal algorithm.

ratio when using acetone as the working fluid as shown above, the acetone is not included in Fig. 20. The recovery rate is 50%. Each line represents a candidate working fluid. The size of the marked points represents the level of operating pressure.

It can be found that for the same working fluid, the augment of the operating pressure will increase the optimal boost ratio. Because the minimal available r increases with the P_{op} increasing and the SEC decreases first and then increases with r increasing as talked above. As the operating pressure increases, the optimal SEC for each working fluid increases. Because the required mechanical work and auxiliary pumps power increase. The booster pump power increases due to the increase of the optimal r. The HP pump power increases due to the growth of the heat source flow.

The optimal scheme of the united operation of the RO components and the conveyor can be obtained based on the results in Fig. 20. The optimal working fluids and boost ratios under different operating pressure are listed in Table 3. It is shown that when the operating pressure is between 5.5~6.0 MPa, the optimal working fluid is R236fa. In the operating pressure of 6.5~7.0 MPa, the optimal working fluid is RC318. When the operating pressure is 7.5~8.0 MPa, the optimal working fluids are R142b and R124, respectively. The optimal boost ratio for each working fluid is listed in Table 3. It is noted that when the freshwater flow is constant, the recovery rate only influences the feed seawater flow of RO components. Thus, the optimal design parameters of the conveyor are determined by the operating pressure.

Fig. 21 shows the optimal SEC of the SRC system, the SRP system and the GBR system under different operating pressure. The recovery rate of the three systems is the same

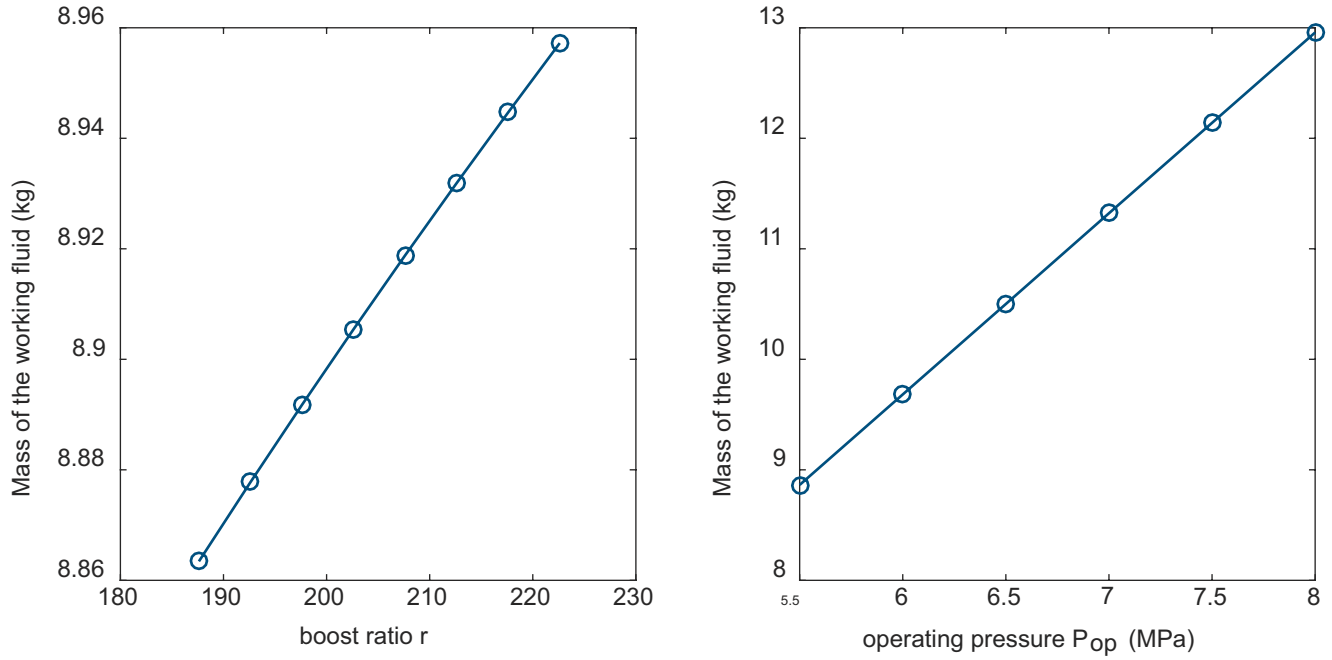

Fig. 14. The filling mass of the working fluid varies with the (a) boost ratio and (b) operating pressure.

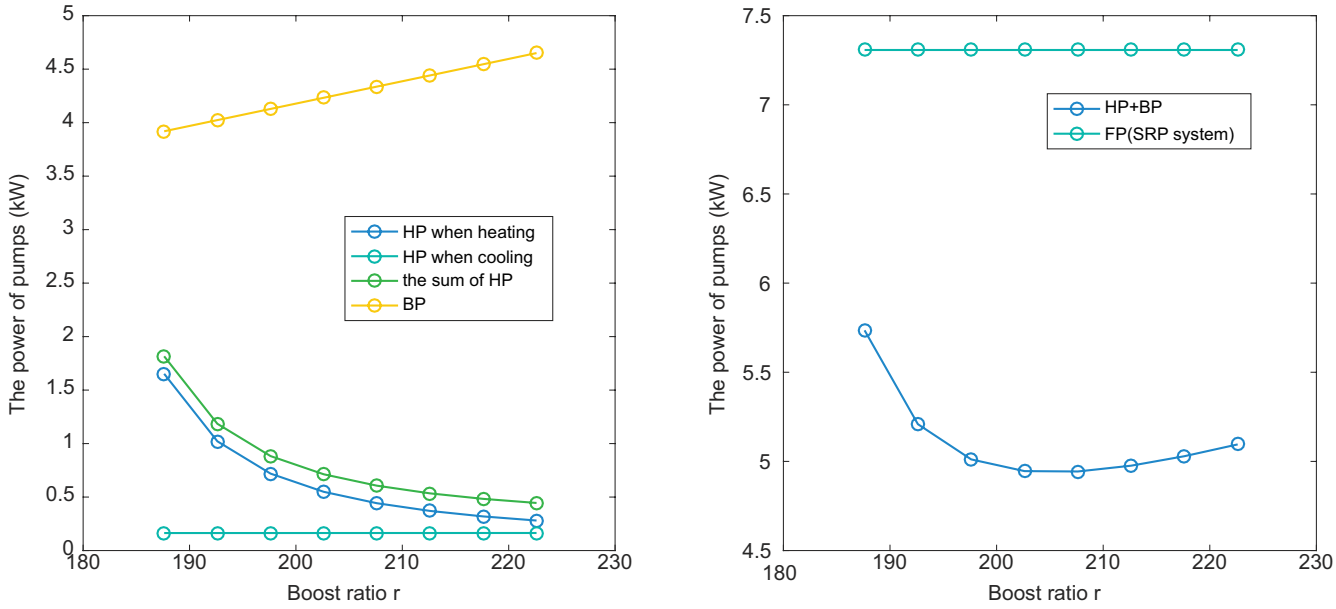

Fig. 15. (a) The power of pumps varies with the boost ratio (P_{op} = 5.5 MPa) and (b) FP power and the sum power of the heat pump and booster pump.

as 50%. As the operating pressure increases, the SEC of three kinds of RO systems increases. The FP head in the SRP system is approximately equivalent to that of the high-pressure pump in the GBR system. While the former has a smaller volume flow, because the freshwater flow is less than the feed seawater flow. Although the SRP system has a circulation pump, its power is small and has little effect on the whole system power. Compared to the GBR system, the SRP system saves about 50% electric energy, which is caused by the participation of seawater hydrostatic pressure in the seawater reverse osmosis process.

The SEC of the SRC system is 1.396 kWh/m^3 at 5.5 MPa, which is 0.527 kWh/m^3 lower than that of the SRP system. The reason is that the sum of the booster pump power and the heat pump power is lower than that of the freshwater pump in the SRP system. In other words, the utilization of

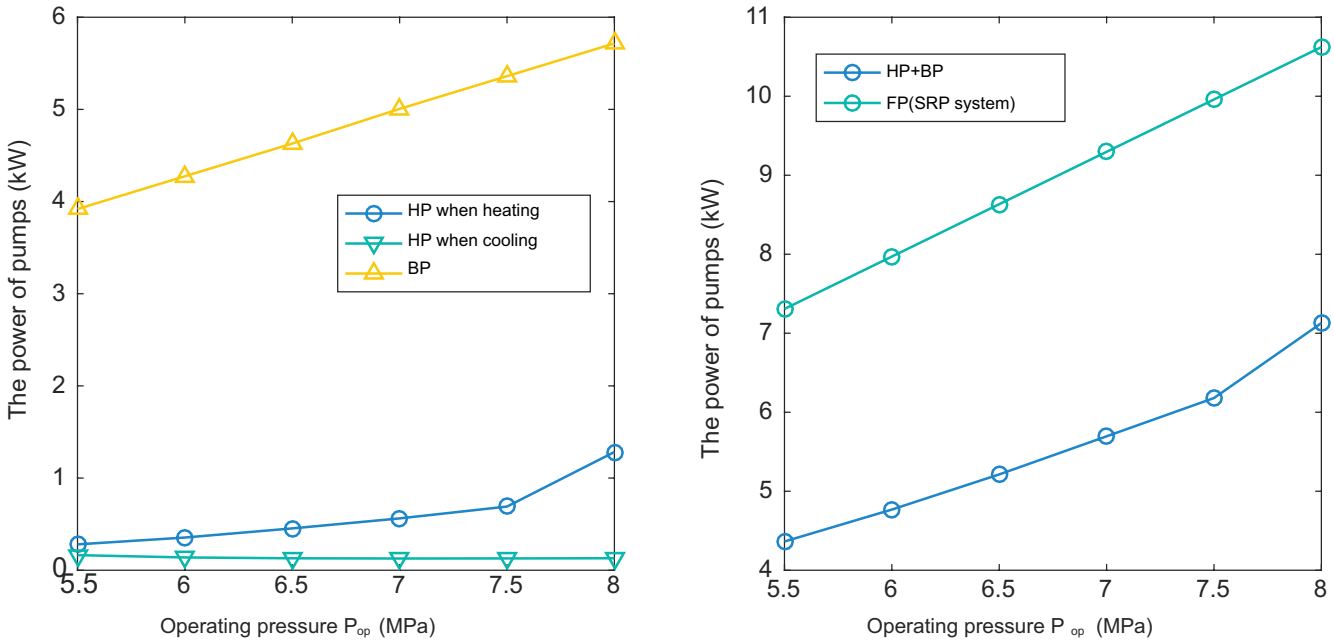

Fig. 16. The power of pumps varies with the operating pressure.

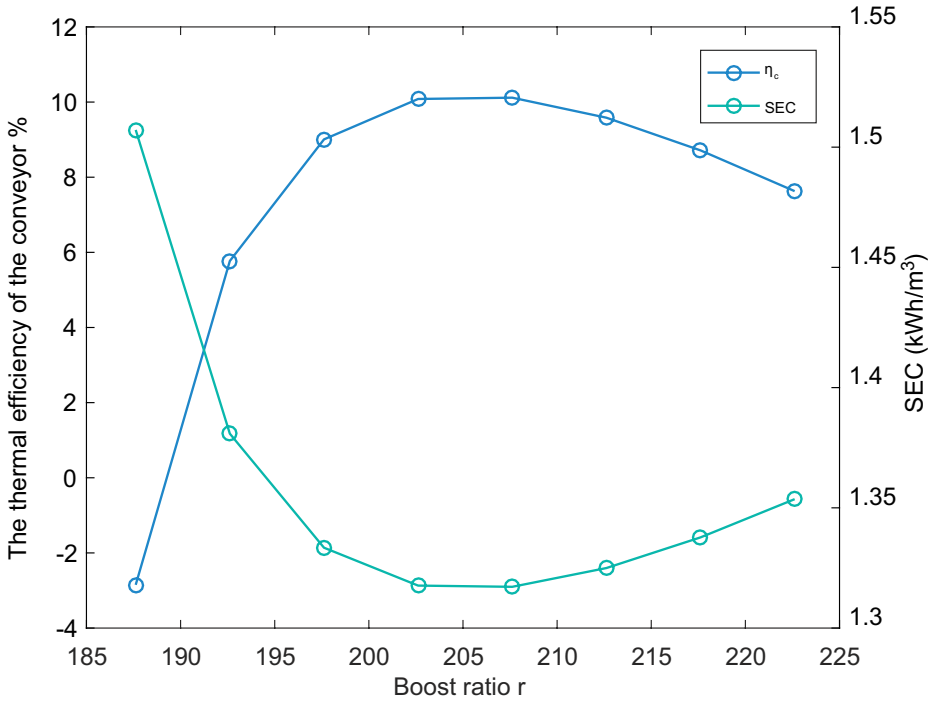

Fig. 17. The thermal efficiency of the conveyor and SEC vary with the boost ratio.

the ocean thermal energy via the conveyor replaced part of the electric energy required in the delivery process.

Research on the RO system that uses hydrostatic pressure as the operating pressure is relatively unpopular. During 1998~2001, Pacenti and Reali et al. [20,23] designed a RODSS (reverse osmosis deep-sea system, same as the SRP system) prototype with the freshwater capacity of 10~12 m^3/d based on the experimental facility in literature [21]. The theoretical SEC of the RODSS system was around 2 kWh/m^3 at the working depth of 550 m and the recovery of 20%~25%. In 2001, a small-production-capacity (10 m^3/d) RODSS prototype desalination unit was tested at the depth of 450 m where was 1 mile off the southwest coast of Pantelleria Island, Sicily and the concept of the RODSS system was verified [22]. In addition, the hydrostatic pressure of a water column of sufficient height

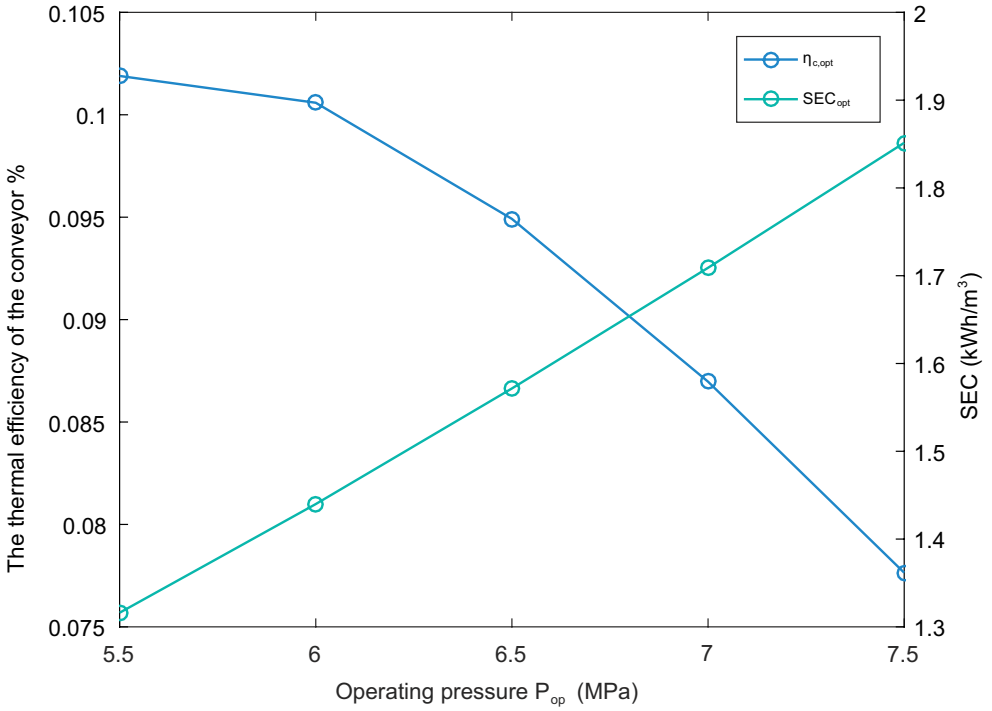

Fig. 18. The thermal efficiency of the conveyor and SEC vary with the operating pressure.

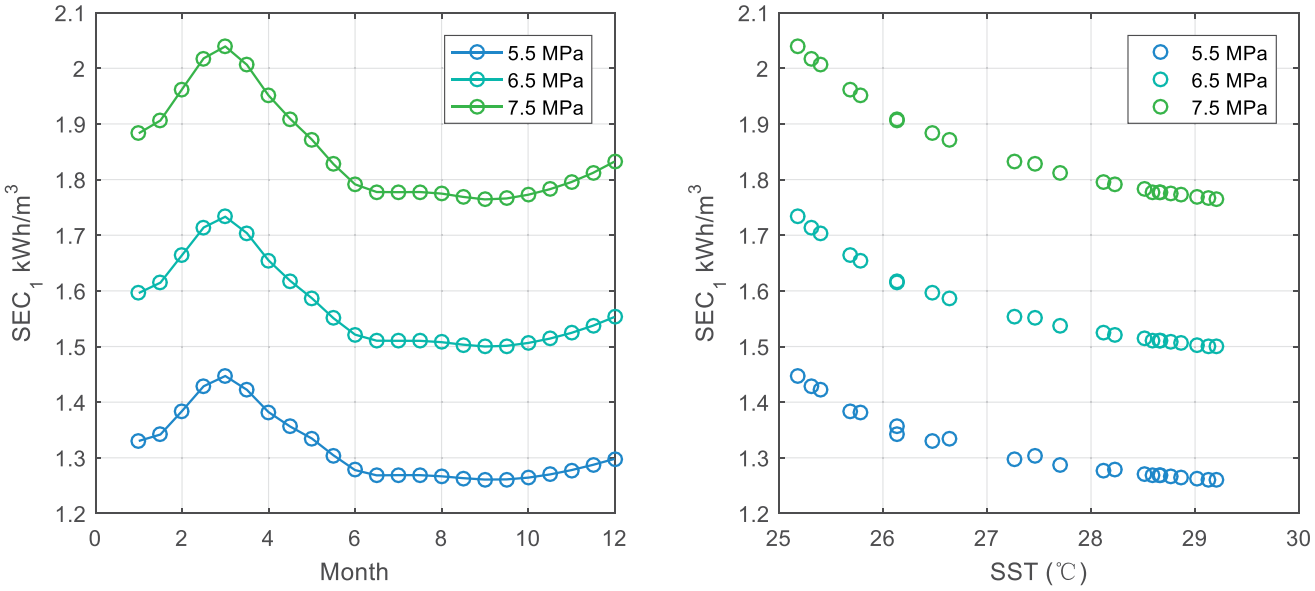

Fig. 19. (a) Monthly SEC varies with the month and (b) monthly SEC varies with SST.

(around 500 m, like a mountain) to create the required pressure to drive the RO desalination system is proposed by Al-Kharabsheh [23]. The theoretical SEC of the system is 0.85~1.4 kWh/m^3 [23,24]. The SRC system is based on the submarine RO system proposed by literature [20–22] and further reduces the SEC by utilizing the ocean thermal energy to deliver the produced freshwater. As shown in Fig. 21, the SEC of the SRP system is 1.923 kWh/m^3, which is consistent with the results in the literature [20,23].

Fig. 22 shows the SEC of the three kinds of systems at different recovery rates when the operating pressure is 7 MPa. As the recovery rate increases, the SEC of the three systems decreases. The reason is that the increase of recovery results in the reduction of the feed seawater flow. Thus, in the submarine RO systems, including the SRP system and SRC system, the power consumption of the circulation pumps would reduce. In the GBR system, the power consumption of the high-pressure pump decreases. It can be

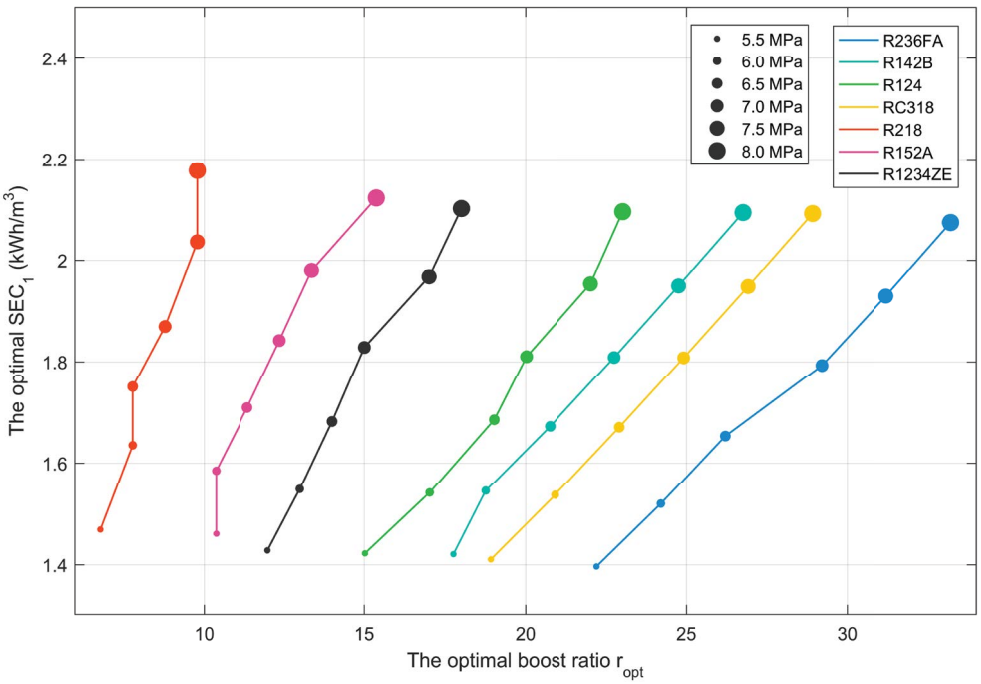

Fig. 20. Optimal boost ratio and corresponding optimal SEC for different working fluids.

Table 3
Optimal design parameters of the SRC system under different working conditions

Operating pressure P_{op} (MPa)	Optimal working fluid	Optimal boost ratio r	Filling mass m_f (kg)	Optimal thermal efficiency η_c (%)	Optimal SEC (kWh m^{-3})
5.5	R236fa	22.21	25.12	4.88	1.39
6.0	R236fa	24.21	27.44	5.16	1.52
6.5	RC318	22.92	39.71	3.87	1.67
7.0	RC318	24.92	42.82	3.48	1.81
7.5	R142b	24.76	22.84	2.92	1.95
8.0	R124	23.03	33.70	2.20	2.10

found that the recovery rate has a greater impact on the SEC of the GBR system. Because the high-pressure pump consumes most of the energy required in the GBR system, while the circulation pumps in the submarine RO systems are not the main electric energy consumption.

Fig. 23 shows the electric energy saving of the SRC system under different operating pressures and recovery rates. The electric energy saving quantitatively reflects the operating cost advantage of the SRC system. When the recovery is the minimum of 10%, the SRC system has the highest electric energy saving of 90% compared to the GBR system. As the recovery increases to 80%, the electric energy saving significantly reduces to about 40%. While compared to the SRP system, the operating cost advantage of the SRC system is slightly enlarged from about 20% to 28% as the recovery increases from 10% to 80%. Therefore, the increase of the recovery can highlight the operating cost advantage compared to the SRP system. But compared to the GBR system, the increase of recovery weakens the operating cost advantage. Electric energy saving compared to the GBR system changes much more obviously than that compared to the SRP system. Because the SEC of the GBR system is influenced sufficiently by the recovery as shown in Fig. 22. In addition, the decrease of the operating pressure can slightly increase the electric energy saving of the SRC system compared to both the SRP system and GBR system. The lower operating pressure of RO components is recommended to be adopted.

6. Comparison with other energy-saving approaches

At present, there are various energy-saving approaches for the SWRO process, while energy-recovery devices (ERDs) are the most mature and widely used. ERD recovers the high pressure of concentrated brine, thereby reducing the power of the high-pressure pump. The SEC of the SWRO-ERD system is around 2.5~4 kWh/m^3 currently [42,43]. In the near future, hybrid systems and high-permeability RO membranes can reduce SEC to 2 kWh/m^3. The

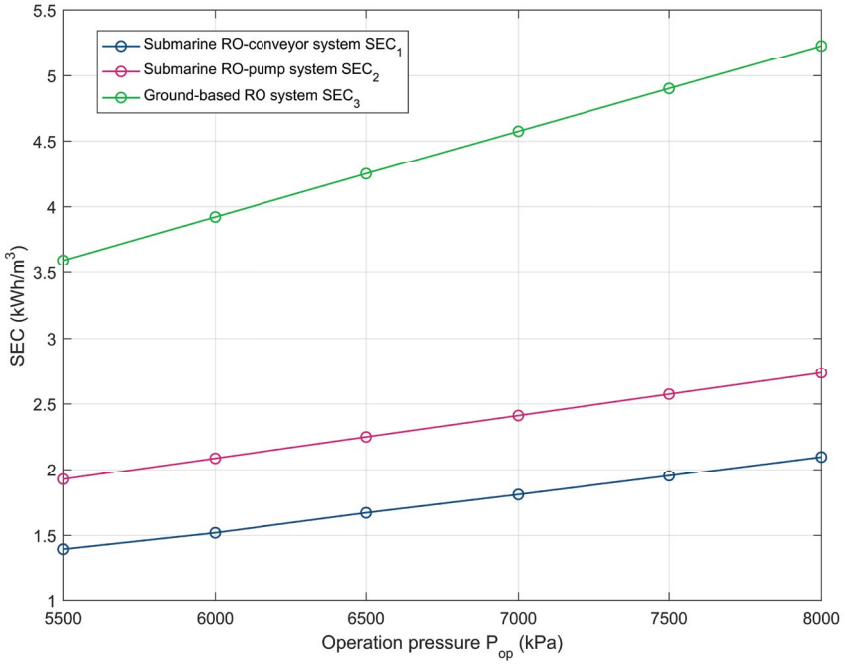

Fig. 21. Comparison of the SEC under different operating pressure.

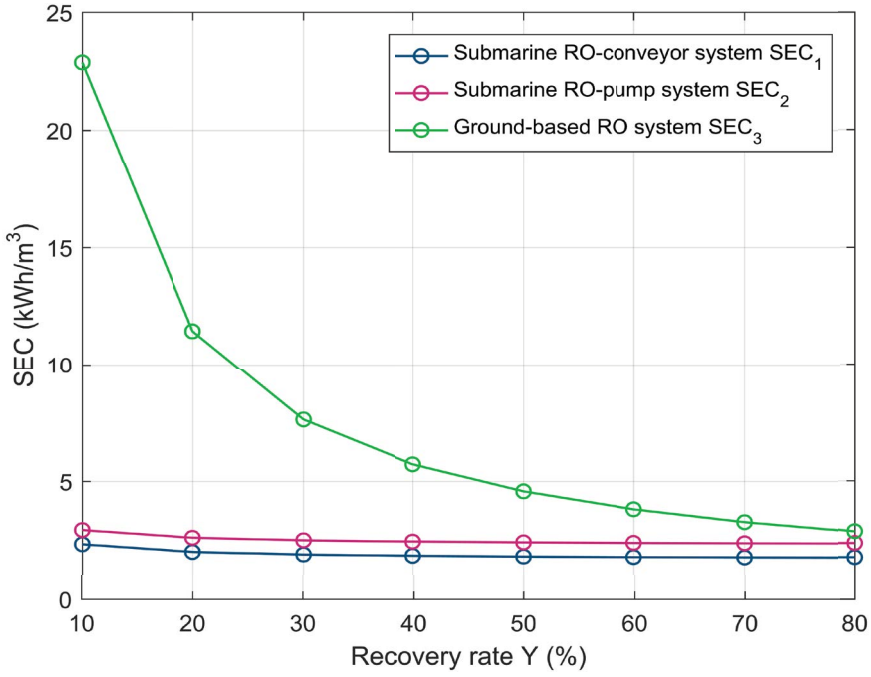

Fig. 22. Comparison of the SEC under different recovery.

combination of forward osmosis processes and low-pressure RO or the combination of the SWRO and pressure retarded osmosis both belongs to the hybrid systems [44,45]. In the more distant future, through other ultrahigh permeability (synthetic water channel or graphene) reverse osmosis membranes, SEC is expected to drop to 1.5 kWh/m^3 [46]. In this work, the theoretical minimum SEC of the proposed system reaches 1.39 kWh/m^3. Therefore, the proposed system could be a potential approach for the RO systems to saving electric energy. However, the SRC system is still in the conceptual design stage. Some practical challenges need to be overcome before practical application. The most critical

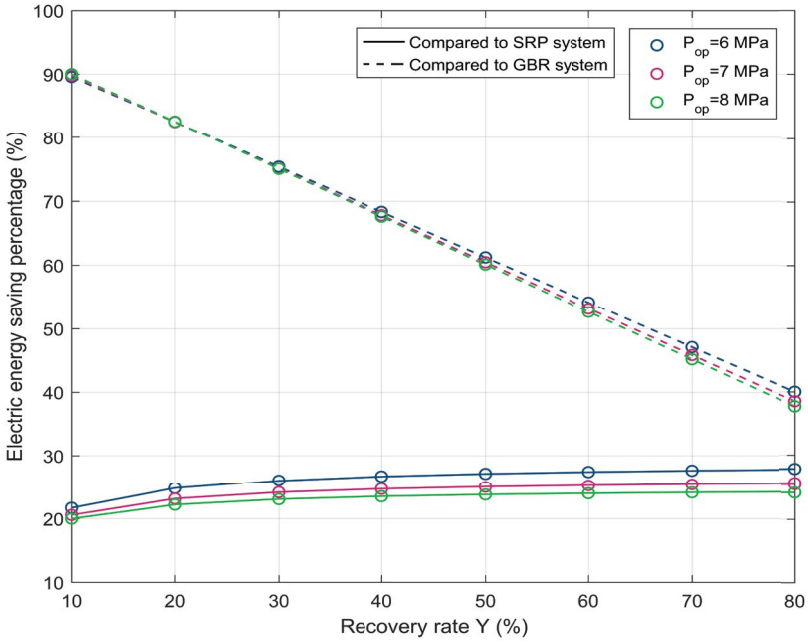

Fig. 23. Variation of the electric energy saving with recovery and operating pressure.

problems we think includes the design of the high-efficiency heat transfer structure of the conveyor and efficient insulation measures on the long-distance pipelines.

7. Conclusion

For the SRC system, the operating pressure of the RO components is provided by the seawater hydrostatic pressure. The conveyor is driven by the temperature difference of the sea surface and the local seawater in the depth of 550~800 m. In order to adapt to the low temperature of the heat source and high evaporation pressure, the pressure boosting mode is adopted in the conveyor. The conclusions are drawn as follows:

- When the operating pressure, recovery rate, working fluids and boost ratio are treated as independent variables. The optimal scheme of the united operation of RO components and the conveyor are obtained under the selected working location as shown in Table 3. The power of the booster pump was the highest and account for around 50% of the total pump power. The SEC increased first and then decreased with the boost ratio growing. With the increase of the operating pressure or the decrease of the recovery rate, the SEC increases. The thermal efficiency and the SEC had opposite trends. Besides, the increase of annual average SST could reduce the SEC, which is derived from the increase of available ocean thermal energy converted by the conveyor. At the typical recovery of 50%, the optimal SEC in this work was obtained as 1.39 kWh/m^3 with the operating pressure of 5.5 MPa. The working fluid was R236fa with a boost ratio of 22.21.
- Compared with the SRP system and the GBR system, the proposed system has the lowest SEC, followed by the SRP system and the highest GBR system. Due to the participation of seawater hydrostatic pressure, the SEC of the SRP system is about 50% lower than that of the GBR system at the typical recovery of 50%. With the assistance of ocean thermal energy, the SEC of the SRC system further reduces by about 20%–30% compared to the SRP system.
- In order to enhance operating cost advantage, it is recommended to choose the lower operating pressure of RO components. In addition, because of the lower temperature of the seawater in the deep sea, the recovery is lower and the life of RO components can be longer. Furthermore, the conveyors could be operated in parallel to increase freshwater production.

Symbols

c	—	Specific heat capacity, J/(kg K)
g	—	Gravity acceleration, m/s^2
D	—	Working depth of the closed container, m
d_n	—	Inner diameter of pipelines
L	—	Length of fresh water pipeline, m
m	—	Mass, kg
n	—	Piston frequency, d^{-1}
P	—	Pressure, Pa
Q	—	Volume flow, m^3/h, or heat flow, W
T	—	Temperature, °C
t	—	Ratio of heating time to cooling time
u	—	Specific thermodynamic energy, J/kg
v	—	Specific volume, m^3/kg
W	—	Power, W
Y	—	Recovery rate of RO membranes, –

Subscripts

1-5	—	Points corresponding to Fig. 2
b	—	Brine or booster pump

c	—	Cold source/cold source pump
cir	—	Circulation pump
co	—	Conveyor
con	—	Condensation
evp	—	Evaporation
F	—	Freshwater pump
f	—	Working fluid/pipe resistance
h	—	Heat source/heat source pump
i	—	Inlet
o	—	Outlet
p	—	Booster pump
RO	—	RO components
s	—	Surface seawater
t	—	Total pumps
w	—	Freshwater
wf	—	Working fluid

Geek alphabet

P	—	Density, kg/m^3
Δ	—	Change value, –
η	—	Pump efficiency/thermal efficiency, –

Acronyms

RO	—	Reverse osmosis
RES	—	Renewable energy sources
SEC	—	Electricity consumption per volume freshwater
SST	—	Surface seawater temperature
SRC	—	Submarine reverse osmosis conveyor
SRP	—	Submarine reverse osmosis-pump
GBR	—	Ground-based reverse osmosis

References

[1] A. Ali, R.A. Tufa, F. Macedonio, E. Curcio, E. Drioli, Membrane technology in renewable-energy-driven desalination, Renewable Sustainable Energy Rev., 81 (2018) 1–21.
[2] B. Peñate, L. García-Rodríguez, Current trends and future prospects in the design of seawater reverse osmosis desalination technology, Desalination, 284 (2012) 1–8.
[3] C. Li, Y. Goswami, E. Stefanakos, Solar assisted sea water desalination: a review, Renewable Sustainable Energy Rev., 19 (2013) 136–163.
[4] M.T. Ali, H.E.S. Fath, P.R. Armstrong, A comprehensive techno-economical review of indirect solar desalination, Renewable Sustainable Energy Rev., 15 (2011) 4187–4199.
[5] A.M. Delgado-Torres, L. García-Rodríguez, Status of solar thermal-driven reverse osmosis desalination, Desalination, 216 (2007) 242–251.
[6] M.W. Shahzad, M. Burhan, L. Ang, K.C. Ng, Energy-water-environment nexus underpinning future desalination sustainability, Desalination, 413 (2017) 52–64.
[7] F. Silva Pinto, R. Cunha Marques, Desalination projects economic feasibility: a standardization of cost determinants, Renewable Sustainable Energy Rev., 78 (2017) 904–915.
[8] M.A. Eltawil, Z. Zhao, L. Yuan, A review of renewable energy technologies integrated with desalination systems, Renewable Sustainable Energy Rev., 13 (2009) 2245–2262.
[9] M.A.M. Khan, S. Rehman, F.A. Al-Sulaiman, A hybrid renewable energy system as a potential energy source for water desalination using reverse osmosis: a review, Renewable Sustainable Energy Rev., 97 (2018) 456–477.
[10] M.G. Buonomenna, J. Bae, Membrane processes and renewable energies, Renewable Sustainable Energy Rev., 43 (2015) 1343–1398.
[11] C. Charcosset, A review of membrane processes and renewable energies for desalination, Desalination, 245 (2009) 214–231.
[12] A. Kasaeian, F. Rajaee, W.-M. Yan, Osmotic desalination by solar energy: a critical review, Renewable Energy, 134 (2019) 1473–1490.
[13] F.E. Ahmed, R. Hashaikeh, N. Hilal, Solar powered desalination – technology, energy and future outlook, Desalination, 453 (2019) 54–76.
[14] A. Mollahosseini, A. Abdelrasoul, S. Sheibany, M. Amini, S.K. Salestan, Renewable energy-driven desalination opportunities – a case study, J. Environ. Manage., 239 (2019) 187–197.
[15] I. Padrón, D. Avila, G.N. Marichal, J.A. Rodríguez, Assessment of hybrid renewable energy systems to supplied energy to autonomous desalination systems in two islands of the Canary Archipelago, Renewable Sustainable Energy Rev., 101 (2019) 221–230.
[16] B.C. Drude, Submarine units for reverse osmosis, Desalination, 2 (1967) 325–328.
[17] P. Glueckstern, Preliminary considerations of combining a large reverse osmosis plant with the Mediterranean—Dead Sea project, Desalination, 40 (1982) 143–156.
[18] C. Charcosset, A review of membrane processes and renewable energies for desalination, Desalination, 245 (2009) 214–231.
[19] D. Hebden, G.R. Botha, On Fresh Water from the Sea, Proc. 6th International Symposium, Bulletin of the Society of Sea Water Science, 1978, p. 197.
[20] M. Reali, M. de Gerloni, A. Sampaolo, Submarine and underground reverse osmosis schemes for energy-efficient seawater desalination, Desalination, 109 (1997) 269–275.
[21] P. Pacenti, M.D. Gerloni, M. Reali, D. Chiaramonti, S.O. Gartner, P. Helm, M. Stohr, Desalination system, Desalination, 126 (1999) 213–218.
[22] D. Colombo, M. de Gerloni, M. Reali, An energy-efficient submarine desalination plant, Desalination, 122 (1999) 171–176.
[23] S. Al-Kharabsheh, An innovative reverse osmosis desalination system using hydrostatic pressure, Desalination, 196 (2006) 210–214.
[24] C. Charcosset, C. Falconet, M. Combe, Hydrostatic pressure plants for desalination via reverse osmosis, Renewable Energy, 34 (2009) 2878–2882.
[25] M.P. Sharma, G. Singh, A low loft solar water pump, Sol. Energy, 25 (1980) 273–278.
[26] K. Sumathy, A. Venkatesh, V. Sriramulu, Thermodynamic analysis of a solar thermal water pump, Sol. Energy, 57 (1996) 155–161.
[27] Y.W. Wong, K. Sumathy, Thermodynamic analysis and optimization of a solar thermal water pump, Appl. Therm. Eng., 21 (2001) 613–627.
[28] K. Sumathy, A. Venkatesh, V. Sriramulu, A solar thermal water pump, Appl. Energy, 53 (1996) 235–243.
[29] Y.W. Wong, K. Sumathy, Performance of a solar water pump with n-pentane and ethyl ether as working fluids, Energy Convers. Manage., 41 (2000) 915–927.
[30] Y.W. Wong, K. Sumathy, Performance of a solar water pump with ethyl ether as working fluid, Renewable Energy, 22 (2001) 389–394.
[31] G.B.de Klerk, C.J. Rallis, A solar powered, back-to-back liquid piston stirling engine for water pumping, J. Energy S. Afr., 13 (2002) 36–42.
[32] D. Debashis, M.R. Gopal, Studies on a metal hydride based solar water pump, Int. J. Hydrogen Energy, 29 (2004) 103–112.
[33] A. Date, A. Akbarzadeh, Theoretical study of a new thermodynamic power cycle for thermal water pumping application and its prospects when coupled to a solar pond, Appl. Therm. Eng., 58 (2013) 511–521.
[34] J. Nihill, A. Date, J. Velardo, S. Jadkar, Experimental investigation of the thermal power pump cycle – proof of concept, Appl. Therm. Eng., 134 (2018) 182–193.
[35] J. Nihill, A. Date, P. Lappas, J. Velardo, Investigating the prospects of water desalination using a thermal water pump coupled with reverse osmosis membrane, Desalination, 445 (2018) 256–265.

[36] G.D. Takalkar, R.R. Bhosale, Mathematical modeling, simulation and optimization of solar thermal powered Encontech engine for desalination, Sol. Energy, 172 (2018) 104–115.
[37] M. Glushenkov, R. Bhosale, A. Kumar, F. AlMomani, Heat Powered Water Pump for Reverse Osmosis Desalination, Proceedings of TechConnect World Innovation Conference & Expo., Materials for Energy, Efficiency and Sustainability, Washington DC, USA, 2016, pp. 201–204.
[38] L.F. Greenlee, D.F. Lawler, B.D. Freeman, B. Marrot, P. Moulin, Reverse osmosis desalination: water sources, technology, and today's challenges, Water Res., 43 (2009) 2317–2348.
[39] A. Poisson, C. Brunet, J.C. Brun-Cottan, Density of standard seawater solutions at atmospheric pressure, Deep Sea Res. Part A, 27 (1980) 1013–1028.
[40] Argo, Argo Float Data and Metadata from Global Data Assembly Centre (Argo GDAC), SEANOE, 2021, doi: 10.17882/42182#61117.
[41] E.W. Lemmon, M.L. Huber, M.O. McLinden, NIST Standard Reference Database 23: Reference Fluid Thermodynamic and Transport Properties-REFPROP, Version 9.0, National Institute of Standards and Technology, Standard Reference Data Program, Gaithersburg, 2010.
[42] M. Tedesco, E. Brauns, A. Cipollina, G. Micale, P. Modica, G. Russo, J. Helsen, Reverse electrodialysis with saline waters and concentrated brines: a laboratory investigation towards technology scale-up, J. Membr. Sci., 492 (2015) 9–20.
[43] G. Amy, N. Ghaffour, Z.Y. Li, L. Francis, R.V. Linares, T. Missimer, S. Lattemann, Membrane-based seawater desalination: present and future prospects, Desalination, 401 (2017) 16–21.
[44] R.V. Linares, Z. Li, S. Sarp, Sz.S. Bucs, G. Amy, J.S. Vrouwenvelder, Forward osmosis niches in seawater desalination and wastewater reuse, Water Res., 66 (2014) 122–139.
[45] S. Zhang, T.-S. Chung, Minimizing the instant and accumulative effects of salt permeability to sustain ultrahigh osmotic power density, Environ. Sci. Technol., 47 (2013) 10085–10092.
[46] M.M. Pendergast, E.M.V. Hoek, A review of water treatment membrane nanotechnologies, Energy Environ. Sci., 4 (2011) 1946–1971.